European Conference on Computational Fluid Dynamics
ECCOMAS CFD 2006
P. Wesseling, E. Oñate, J. Périaux (Eds)

USE OF POD IN CONTROL OF FLOW THROUGH POROUS MEDIA

Jorn van Doren*†, Renato Markovinović* and Jan-Dirk Jansen*‡

* Delft University of Technology, Department of Geotechnology,
PO Box 5028, 2600 GA, Delft, The Netherlands.
E-mail: j.f.m.vandoren@dcsc.tudelft.nl

† Delft University of Technology, Delft Center for Systems and Control (b8C-3-10)
Mekelweg 2, 2628 CD, Delft, The Netherlands

‡Shell International Exploration and Production, Exploratory Research
PO Box 60, 2280 AB Rijswijk, The Netherlands.

Key words: proper orthogonal decomposition, model reduction, optimal control, reservoir engineering, porous media, water flooding

Abstract. *During the design of development concepts for the exploitation of oil and gas reservoirs, frequent use is made of numerical simulation of the flow of multi-phase fluids through porous rock. Recently, increased attention has been paid to systematic optimization of well positions and operating parameters (rates, pressures) over the life of the reservoir. Here we consider optimization of the displacement of oil towards production wells through the injection of water in other wells. Model-based optimal control of this "water flooding" process generally involves multiple simulations, which makes it into a time-consuming process. A potential way to address this issue is through the use of proper orthogonal decomposition (POD), We addressed the scope to speed up optimization of water-flooding a heterogeneous reservoir with multiple injectors and producers. We used an adjoint-based optimal control methodology that requires multiple passes of forward simulation of the reservoir model and backward simulation of an adjoint system of equations. We developed a nested approach in which POD was first used to reduce the state space dimensions of both the forward model and the adjoint system. After obtaining an optimized injection and production strategy using the reduced-order system, we verified the results using the original, high-order model. If necessary, we repeated the optimization cycle using new reduced-order systems based on snapshots from the verification run We tested the methodology on a reservoir model with 882 states (441 pressures, 441 saturations) and an adjoint model of 882 states (Lagrange multipliers). We obtained reduced-order models with 35-43 states only. The reduction in computing time was 52%.*

1 INTRODUCTION

An important aspect of the development of oil and gas reservoirs involves the numerical simulation of multi-phase fluid flow through porous rock. The governing differential equations can be derived from the mass balance equations for the components of the reservoir fluids, the equations of state for the phase behavior, and a semi-empirical relation, known as

Darcy's law, which describes the relation between pressure drop and fluid velocity[1,2]. Reynolds numbers are typically much smaller than one, and inertia effects are therefore disregarded. However, capillary forces and the mutual interference of the various phases (oil, gas, water) result in nonlinearities that complicate the analysis. Here, we restrict ourselves to the flow of oil and water, in which case we can obtain the governing equations as two coupled differential equations that are of second order in space and of first order in time. Under some mild assumptions they can be expressed as a weakly nonlinear parabolic equation with time-varying coefficients for the pressure field, coupled to a strongly nonlinear hyperbolic-parabolic equation for the phase saturation field. Discretization in space is mostly done using finite differences with upstream weighting for the saturation-dependent parameters. The most popular time-stepping schemes are fully implicit Euler integration using Newton iteration, or a combination of implicit pressure integration and explicit saturation updates. Here we use a semi-implicit integration, i.e. implicit in the primary variables (pressures and saturations) but explicit in the saturation-dependent parameters. Typical reservoir models contain 10^4 - 10^6 grid blocks and take many hours to run. The major use of such models is in the design phase of field development, to predict the performance of alternative development schemes. This involves the positioning of the wells and assessment of the effectiveness of different recovery techniques. Most oil fields initially produce oil naturally because of the high subsurface pressure, but this "primary recovery" phase usually ends because of a decreasing reservoir pressure with increasing cumulative hydrocarbon production. Typically, at the end of this phase 70% to 95% of the oil is still left in the reservoir. A "secondary recovery phase" is then entered during which the reservoir pressure is maintained or restored through the injection of gas or water. In addition to pressure maintenance, the injected fluids help to displace the oil from the injection wells to the production wells. Several authors investigated the scope to optimize the design of secondary recovery through combining reservoir simulation with systematic optimization techniques. In particular the scope to optimize oil recovery through water injection, a recovery technique known as "water flooding" has been studied using optimal control theory (OCT)[3,4,5]. The objective functions in these studies were either oil recovery or monetary value, and the controls were the injection and production rates of the wells over the entire life of the reservoir. OCT is a gradient-based local optimization technique where the derivative information is obtained through solving a set of adjoint differential equations backward in time. At the price of having to derive the adjoint equations, OCT provides a computationally efficient means to obtain the derivatives of the objective function with respect to all control parameters in a single set of forward and adjoint simulations. Over the past years, the interest in OCT for flooding optimization has increased because of the development of "smart" horizontal wells, equipped with downhole sensors and downhole valves that allow for individual control of the inflow or injection from different segments of the wells[6,7]. Calculating the optimal valve settings using OCT requires several passes of forward simulation of the reservoir model and backward simulation of the adjoint system of equations. The time needed to calculate optimized controls increases with the number of grid blocks and the complexity of the reservoir model. Reduced-order modeling and reduced-order control may provide a means to reduce the computational burden. Moreover, the use of reduced-order models may also lead to accelerated convergence in

iterative solutions. In this paper we concentrate on the use of proper orthogonal decomposition (POD)[8]. POD, also known as principal component analysis, Karhunen-Loève decomposition or the method of empirical orthogonal functions, is a frequently used tool for model reduction but only recently it has been used for control applications[9,10,11,12]. Moreover its application to the simulation of flow through porous media has also been scarce[13,14,15,16]. In this paper we will describe a methodology using nested loops, where the inner iterative loop makes use of a truncated basis of POD functions to calculate optimized injection and production rates. After convergence in this loop we simulate in the outer loop the original, high-order model with the optimized rates and subsequently adapt the basis and the truncation of the POD functions. They are used in the next inner loop to calculate new optimized injection and production rates. We published the theory behind this methodology earlier, and illustrated it with a numerical example[17]. More recently we developed a different approach to use POD for the improvement of computational efficiency in reservoir simulation[18]. Here we will present a shortened version of the theory from the former publication and an application to a different, simple two-dimensional water flooding example.

2 HIGH-ORDER RESERVOIR MODEL

To generate a reduced-order model with POD we first need to run a full-order simulation and produce snapshots. For the full-order model we use a two-dimensional, two-phase, reservoir simulator based on a spatial finite difference discretization of the governing flow equations, which can be represented as a set of coupled nonlinear differential equations in continuous time t:

$$\dot{\mathbf{x}}(t) = \mathbf{A}(\mathbf{x})\mathbf{x}(t) + \mathbf{B}(\mathbf{x})\mathbf{u}(t) \quad . \tag{1}$$

Here, $\mathbf{x}$ is the n-dimensional state vector containing oil pressures p_o and water saturations S_w for each grid block, $\mathbf{A}$ and $\mathbf{B}$ are saturation-dependent matrices and $\mathbf{u}$ is the input vector containing water rates q_w at the injectors and liquid (i.e. the sum of oil and water) rates $q_l = q_o + q_w$ at the producers. We choose Neumann (no-flow) boundary conditions around the entire domain, while the initial conditions are specified as $\mathbf{x}(0) = \mathbf{x}_0$. Implicit Euler discretization can be written as,

$$\frac{\mathbf{x}(k+1) - \mathbf{x}(k)}{\Delta t} = \mathbf{A}(\mathbf{x}(k))\mathbf{x}(k+1) + \mathbf{B}(\mathbf{x}(k))\mathbf{u}(k), \tag{2}$$

resulting in the nonlinear system of equations

$$\left[\mathbf{I} - \Delta t\mathbf{A}(\mathbf{x}(k))\right]\mathbf{x}(k+1) = \mathbf{x}(k) + \Delta t\mathbf{B}(\mathbf{x}(k))\mathbf{u}(k), \tag{3}$$

where k is discrete time. By solving system (3) every time step without iteration on the saturation-dependent parameters in $\mathbf{A}$ and $\mathbf{B}$ we obtain a semi-implicit time stepping scheme, with a stability limit governed by the throughput limit of the grid blocks[1].

3 PROPER ORTHOGONAL DECOMPOSITION

An approximation of the system dynamics is obtained by projecting the original n-dimensional state space onto an l-dimensional subspace. First, during simulation of an n-dimensional discrete-time model we record a total of κ snapshots for the oil pressure state $\mathbf{x}_p$ and the water saturation state $\mathbf{x}_s$. In our case the dimension n is equal to twice the number of grid blocks. We keep the pressure and the saturation states segregated because they correspond to different physical processes and will consequently generate different dominant structures. Moreover, it allows us to choose a different degree of reduction for the pressures and the saturations. For clarity of notation, we will omit the indication of pressure or saturation for the variables in this section, but we note that all steps in the order reduction process should be performed twice, once for the pressures and once for the saturations. After subtracting the mean $\overline{\mathbf{x}} = (1/\kappa)\sum_{i=1}^{\kappa} \mathbf{x}(i)$ from the snapshots, we construct a data matrix:

$$\mathbf{X} := \left[\mathbf{x}'(1),\ \mathbf{x}'(2),\ ...,\ \mathbf{x}'(\kappa)\right] = \left[\mathbf{x}(1) - \overline{\mathbf{x}},\ \mathbf{x}(2) - \overline{\mathbf{x}},\ ...,\ \mathbf{x}(\kappa) - \overline{\mathbf{x}}\right]. \tag{4}$$

The goal of POD is, given the data matrix $\mathbf{X}$, to find a transformation

$$\mathbf{x}' = \mathbf{\Phi}_l \mathbf{z} + \mathbf{r} \tag{5}$$

where $\mathbf{\Phi}_l$ is an $n \times l$ transformation matrix, $\mathbf{z}$ is a reduced state vector of length l and $\mathbf{r}$ are residuals, such that the squared sum of the snapshot residuals, $\sum_{i=1}^{\kappa} \left\|\mathbf{r}(i)\right\|^2$, is minimized. It can be shown, that this minimum is given by

$$\sum_{i=1}^{\kappa} \left\|\mathbf{r}(i)\right\|^2 = \sum_{j=l+1}^{\kappa} \lambda_j \tag{6}$$

where $\lambda_1 \geq \lambda_2 \geq \ldots \geq \lambda_\kappa \geq \lambda_{\kappa+1} = \ldots = \lambda_n = 0$ are the ordered solutions of the eigenvalue problem

$$\mathbf{R}_n \boldsymbol{\varphi}_i = \lambda_i \boldsymbol{\varphi}_i \tag{7}$$

and $\boldsymbol{\varphi}_i$ $(i = 1, \ldots, n)$ are the corresponding eigenvectors. According to equation (6) the squared sum of the snapshot residuals is determined by the $\kappa - l$ highest eigenvalues. The eigenvectors corresponding to the remaining l eigenvalues, i.e. the first l columns of matrix $\mathbf{\Phi}$, form the optimal transformation matrix $\mathbf{\Phi}_l$. We may, alternatively, compute the eigenvectors $\boldsymbol{\varphi}$ with the aid of the singular value decomposition (SVD) of the data matrix[19]:

$$\mathbf{X} = \mathbf{\Phi \Sigma \Psi}^T \tag{8}$$

where the $n \times \kappa$ matrix $\mathbf{\Sigma}$ is given by

$$\mathbf{\Sigma} = \begin{bmatrix} \sigma_1 & 0 & \cdots & 0 \\ 0 & \sigma_2 & \cdots & 0 \\ \vdots & \vdots & \ddots & \vdots \\ 0 & 0 & \cdots & \sigma_\kappa \\ \vdots & \vdots & \ddots & \vdots \\ 0 & 0 & \cdots & 0 \end{bmatrix}, \tag{9}$$

Here $\sigma_1 \geq \ldots \geq \sigma_l >> \sigma_{l+1} \geq \ldots \geq \sigma_\kappa \geq 0$ are the singular values of $\mathbf{X}$ and are the square roots of the eigenvalues λ_i, $i = 1, 2, \ldots, \kappa$. The number of singular values l, i.e. the number of POD basis functions that we want to keep can now be determined as follows. The total amount of relative 'energy' present in the snapshots can be expressed as $E_{tot} = \sum_{i=1}^{\kappa-1} \sigma_i^2$. The reduced number of basis functions is the largest number $l \in \{1, \ldots, \kappa - 1\}$ that satisfies

$$E = \frac{\sum_{i=1}^{l} \sigma_i^2}{E_{tot}} \leq \alpha, \tag{10}$$

where α denotes the fraction of relative energy we want to be captured. If the singular values, ordered by magnitude, display a clear drop, the system apparently has a natural set of dominant singular values. Otherwise, the choice of α becomes somewhat arbitrary. Frequently used cut-off levels are $0.9 < \alpha < 1.0$. The transformation matrix $\mathbf{\Phi}_l$ is now taken as the first l columns of the matrix $\mathbf{\Phi}$, and we obtain the transformation:

$$\mathbf{x} \simeq \mathbf{\Phi}_l \mathbf{z} + \overline{\mathbf{x}} \tag{11}$$

4 REDUCED-ORDER RESERVOIR MODEL

After replacing the $\simeq$ sign by the = sign, and dropping the subscript l to simplify the notation, we can substitute relation (11) into equation (3) to obtain

$$\left[\mathbf{I} - \Delta t \mathbf{A}\left(\mathbf{\Phi}\mathbf{z}(k) + \overline{\mathbf{x}}\right)\right]\mathbf{\Phi}\mathbf{z}(k+1) = \mathbf{\Phi}\mathbf{z}(k) + \Delta t \mathbf{B}\left(\mathbf{\Phi}\mathbf{z}(k) + \overline{\mathbf{x}}\right)\mathbf{u}(k) \tag{12}$$

This transformation can be interpreted as a system of discrete-time differential equations in reduced-order state space, obtained by projecting the normalized state vector $\mathbf{x}' = \mathbf{x} - \overline{\mathbf{x}}$ of the original problem on the reduced-order space. In our implementation we successfully used

$$\underbrace{\mathbf{\Phi}^T\left[\mathbf{I} - \Delta t \mathbf{A}_c\left(\mathbf{\Phi}\mathbf{z}(k) + \overline{\mathbf{x}}\right)\right]\mathbf{\Phi}}_{lxl}\mathbf{z}(k+1) = \mathbf{z}(k) + \mathbf{\Phi}^T \Delta t \mathbf{B}_c\left(\mathbf{\Phi}\mathbf{z}(k) + \overline{\mathbf{x}}\right)\mathbf{u}(k), \tag{13}$$

which is obtained from equation (12) by pre-multiplying with $\mathbf{\Phi}^T$. The number of state variables is thus reduced from n to $l = l_p + l_s$. Note that we now use the variable l to indicate

the *total* number of reduced state variables. The matrix dimensions for the total system are consequently reduced from $n \times n$ to $l \times l$. The simulation time of the reduced-order model using semi-implicit discretization is decreased because we have to solve l equations instead of n equations in the full-order model, where $l << n$. For fully-implicit simulation where more than one systems of equations have to be solved during every time step the decrease in simulation time is expected to be even higher. Unfortunately, the original penta-diagonal matrix structure is changed to a full matrix, because we multiply the penta-diagonal matrix with a full matrix $\mathbf{\Phi}$ from the left side and from the right side. This counteracts the computational advantage obtained by reducing the size of the state vector. When we simulated reduced-order reservoir models with the same controls as the original full-order models we obtained almost identical states, as long as a sufficient fraction of the relative energy of the full-order model was preserved. However, when we strongly altered the controls, and therefore the structures of the states, the states of the full-order model were less well represented by the reduced-order model. Because it is not possible to specify a priori the validity of a reduced-order model, we will use a nested approach in the development of the optimization methodology below, such that the reduced-order results are frequently validated by the full-order model.

5 REDUCED-ORDER OPTIMAL CONTROL

Adjoint-based OCT is an effective technique to optimize the settings of control variables $\mathbf{u}(k)$ over the life of the reservoir to maximize an objective function $J = \sum_{k=1}^{K} J_k\left(\mathbf{x}(k), \mathbf{u}(k)\right)$. OCT is a gradient-based optimization technique, where the gradients are obtained with the aid of an adjoint equation in terms of Lagrange multipliers $\boldsymbol{\lambda}$. The multipliers represent the objective function's sensitivities to changes in the state variables and originate from adding the dynamic system as a constraint to the objective function. In our application, the controls are formed by the injection and production rates in the smart well segments at every time step. Following the derivation in reference [6], the adjoint equation can be written as in discrete time as

$$\boldsymbol{\lambda}(k)^T \left(\frac{\partial \mathbf{g}(k-1)}{\partial \mathbf{x}(k)} \right) = \left[-\boldsymbol{\lambda}(k+1)^T \frac{\partial \mathbf{g}(k)}{\partial \mathbf{x}(k)} - \frac{\partial J_k(k)}{\partial \mathbf{x}(k)} \right], \tag{14}$$

where

$$\mathbf{g}(k) = \left[\mathbf{I} - \Delta t \mathbf{A}\left(\mathbf{x}(k)\right) \right] \mathbf{x}(k+1) - \mathbf{x}(k) - \Delta t \mathbf{B}\left(\mathbf{x}(k)\right) \mathbf{u}(k) = \mathbf{0} \tag{15}$$

is a compact representation of the system equations (3). For our implementation, instead of using the full-order model, we added the reduced-order model as a constraint to the objective function J with the aid of a set of low-order Lagrange multipliers $\boldsymbol{\mu}$:

$$\overline{J}_{red} = \sum_{k=0}^{K-1} \left[J_k\left(\mathbf{\Phi z}(k), \mathbf{u}(k)\right) + \boldsymbol{\mu}(k+1)^T \mathbf{\Phi}^T \mathbf{g}\left(\mathbf{\Phi z}(k+1), \mathbf{\Phi z}(k), \mathbf{u}(k)\right) \right], \tag{16}$$

where we note that we need to add $\bar{\mathbf{x}}$ to each product $\mathbf{\Phi z}$, in line with equation (11). Taking the first variation of Eq. 16, and reworking the results, we obtain a reduced-order equation in terms of reduced-order Lagrange multipliers:

$$\left(\boldsymbol{\mu}(k)\right)^T \underbrace{\left(\mathbf{\Phi}^T \frac{\partial \mathbf{g}(k-1)}{\partial \mathbf{x}(k)} \mathbf{\Phi}\right)}_{lxl} = \left[-\left(\boldsymbol{\mu}(k+1)\right)^T \underbrace{\left(\mathbf{\Phi}^T \frac{\partial \mathbf{g}(k)}{\partial \mathbf{x}(k)} \mathbf{\Phi}\right)}_{lxl} - \underbrace{\left(\frac{\partial J_k(k)}{\partial \mathbf{x}(k)} \mathbf{\Phi}\right)^T}_{1xl} \right], \tag{17}$$

Starting from the final condition $\boldsymbol{\mu}(K)^T = \mathbf{0}$ it can be integrated backward in time. Because the derivatives in Eq. (17) consist of state-dependent parameters we first calculate the full-order derivatives. They are then transformed and reduced by projecting them on the axes of the low-order model. After calculating $\boldsymbol{\mu}$ every time step we can calculate:

$$\frac{\partial \mathcal{L}(k)}{\partial \mathbf{u}(k)} = \frac{\partial J_k(k)}{\partial \mathbf{u}(k)} + \boldsymbol{\mu}(k+1)^T \left\{ \mathbf{\Phi}^T \frac{\partial \mathbf{g}(k)}{\partial \mathbf{u}(k)} \right\}. \tag{18}$$

We compute improved controls using a steepest ascend method according to $\mathbf{u}_{new} = \mathbf{u}_{old} + \varepsilon \, \partial \mathcal{L}(k) / \partial \mathbf{u}(k)$ where ε is a weight factor. The computational advantage of using reduced-order models in OCT is that the system of equations involves only *l* unknowns, whereas the original system involved *n* unknowns. This decreases the simulation time considerably, especially for large systems where $l << n$. Unfortunately, the original block penta-diagonal matrix structure of $\partial \mathbf{g}(k-1) / \partial \mathbf{x}(k)$ and the block-diagonal matrix structure of $\partial \mathbf{g}(k) / \partial \mathbf{x}(k)$ are changed to full matrices, because we multiply them with full matrices $\mathbf{\Phi}$ and $\mathbf{\Phi}^T$. This counteracts the computational advantage obtained by using reduced-order optimal control.

6 METHODOLOGY

The implementation of the full-order OCT algorithm for water flooding was described in reference [6]. In reduced-order optimal control based on POD (see Figure 1) we first simulate the dynamical behavior of the system over time interval 0 to *K* with an initial choice of **u** and compute the NPV. Following reference [6], the initial choice of **u** reflects a flooding strategy with constant rates in the wells. Every time step we record and store a total of κ snapshots of pressures and saturations and calculate POD transformation matrices $\mathbf{\Phi}$. Now instead of using the full-order derivatives of the system we use the reduced-order derivatives for the backward calculation and calculate $\boldsymbol{\mu}$ with Eq. (17). Based on the derivatives computed with Eq. (18) we compute new controls and use them for the next reduced-order forward simulation. For this simulation we use the same transformation matrices $\mathbf{\Phi}$. This means that the computational 'overhead' of calculating $\mathbf{\Phi}$ is shared by multiple runs of the reduced-order model. To determine convergence of the inner loop we use a convergence criterion *c*. The inner loop has converged when the NPV of a reduced-order forward simulation is less than *c* times the NPV

of the previous reduced-order simulation. Convergence of the inner loop may occur because a local maximum of the NPV has been reached or because the controls have changed too much to be accurately captured in the reduced system representation. Entering the outer loop again we use the improved controls in a full-order forward simulation and verify if the controls have indeed maximized the NPV. If necessary, the transformation matrices $\mathbf{\Phi}$ are replaced with new ones that reflect the altered dynamics and the inner loop is repeated. The outer loop has converged when the NPV of the full-order forward simulation is less than the NPV of the previous full-order simulation.

We implemented the methodology in a MATLAB algorithm. The advantage of the methodology is that we use reduced-order forward simulations and reduced-order optimal control, which have a shorter simulation time. A disadvantage is that an improved control of the reduced-order model is not necessarily an improved control for the full-order model. In the numerical example below we will see that in our example this is, however, not a problem. Assessment of the robustness of this approach requires further research on more realistic reservoir models.

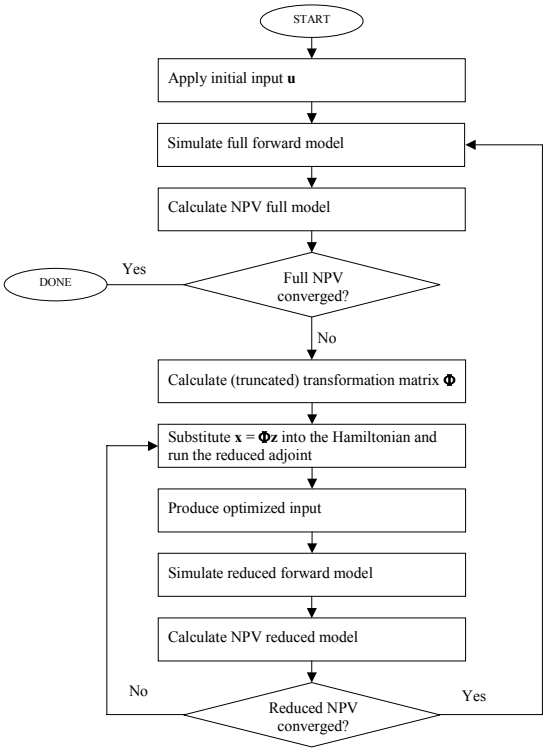

Figure 1: Flow chart for reduced-order OCT for water flooding

7 NUMERICAL EXAMPLE

The methodology as described in the previous section was tested on a 2-dimensional model with 21x21 grid blocks, where each grid block is 10x10x10 m. The permeability field is assumed to be known and is shown in Figure 2. We assign liquid compressibilities to water

and oil of 1×10^{10} Pa^{-1}. Before production, the reservoir is saturated with oil except for a small amount of "connate" water, and it is assumed that all wells start production and injection at the same time. In total nine wells are introduced and they are organized in a nine-spot. This means that we have four producer wells in the corners of the reservoir and one producer well in the middle of the reservoir. Between the producer wells at the corners and the producer well in the center are four injectors. The wells operate under rate-constraint and the total production and injection rates are equal to each other during the entire simulation time. The objective function represents a simple NPV, defined as the sum of the incremental discounted oil production income and water production costs over the life of the reservoir. In the NPV calculation we use an oil price r_o = \$80/m^3 and a produced water cost r_w = \$20/m^3. We compare the NPV obtained with the reduced-order and full-order optimal control algorithms with the NPV of a reference case. In the reference case the injection and production rates are constant over time and a function of water and oil mobility, reflecting a conventional water flood where the wells are operated at constant bottom hole pressure. We simulate the reservoir model for 900 days with variable time step size and in this period we inject and produce one pore volume of liquid. The resulting saturation distribution is depicted in Figure 3. The total NPV for the reference case is \$ 3.0 million. It can be seen that the water saturation (red) around the injector wells is high and the water is pushing the oil towards the producer wells in the center and in the corners.

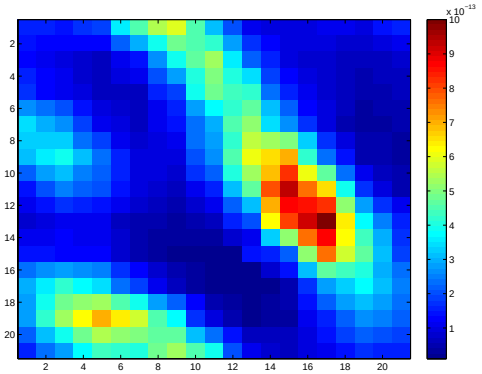

Figure 2: Permeability field (m^2).

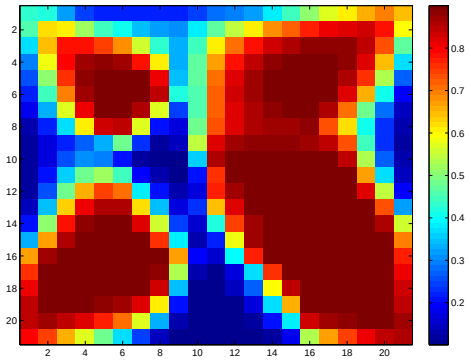

Figure 3: Final water saturation after 1 pore volume of injection and production for the reference case. Red: oil; blue: water.

7.1 Full-order optimal control example

Starting from the reference case we ran the full-order control algorithm. With a 1.86 Gh Pentium M processor and 1 Gb RAM memory it took 950 s to run the full-order algorithm. We reached convergence after 24 full-order forward simulations and 23 full-order backward simulations. The average simulation time for the full-order forward simulation was 12 s and for the full-order backward simulation 24 s, approximately a factor of 2 slower. The resulting optimized rates are given in the left and the middle picture of Figure 4, which correspond to a

final oil/water saturation distribution as depicted in the right picture of Figure 4. The maximum value of the NPV is $4.5 million and in further iterations the NPV is not increasing anymore. The maximum value for NPV should be regarded as a lower bound of the possible improvements, because our optimization routine is local.

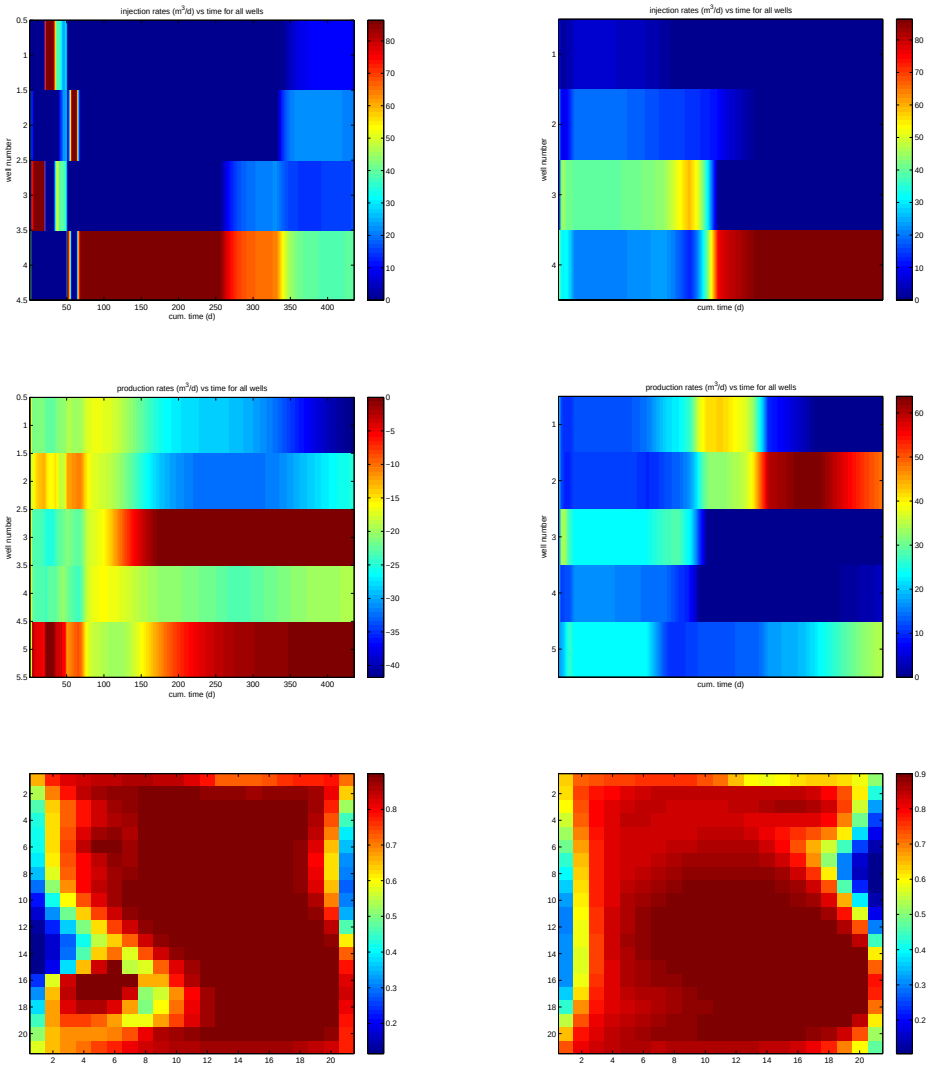

Figure 4: The three pictures in the left column are generated with full-order optimal control: the picture top left represents optimized injection rates for all four injectors (m^3/d vs. the simulation time), the picture middle left production rates for all five producers (m^3/d vs. the simulation time), and the picture bottom left the resulting water saturation distribution (Red: oil; blue: water). The three pictures in the right column are generated with reduced-order optimal control: the picture top right represents optimized injection rates (m^3/d vs. the simulation time), the picture middle right production rates (m^3/d vs. the simulation time), and the picture bottom right the resulting water saturation distribution (Red: oil; blue: water).

7.2 Reduced-order optimal control example

To illustrate reduced-order optimal control we test the methodology as described in Section 6, starting from the reference case. Using a cut-off criterion of 0.999 convergence is reached after 450 s, which is a reduction with 52 % of the time used for the full-order optimal control. With this cut-off level we obtain a maximum NPV of $ 4.42 million, which is an increase of 46% with respect to the reference case. In order to maintain an energy level of 0.999 we need for the reference case 35 POD basis functions. The number of POD basis functions gradually increases when we apply improved controls and for the optimal case we need 43 POD basis functions. This speaks in favor of our nested approach where we adapt the transformation matrix after a full-order forward simulation. The resulting rates for this case are given in the right part of Figure 4. The resulting rates and the final saturation distribution obtained with reduced-order optimal control differed from the resulting rates and final saturation distribution obtained with full-order optimal control. Apparently we end up in two different optima. The maximum NPV obtained with reduced-order control approaches the NPV obtained with full-order optimal control within 99%.

8 CONCLUSIONS

In the example discussed we found that reduced-order optimal control of water flooding using POD improved the NPV with respect to an uncontrolled reference case. Within a shorter simulation time, the NPV obtained by the full-order optimal control algorithm was approached closely by the NPV obtained by the reduced-order algorithm. The increase in computational efficiency was achieved by reducing the number of states in the forward and backward simulations considerably and consequently the number of equations that needed to be solved every time step. Considering a reservoir model with 882 states (441 pressures, 441 saturations) and an adjoint model of 882 states (Lagrange multipliers) we obtained reduced-order models with 35-43 states only. The NPV obtained by reduced-order optimal control was approached to within 99% of the NPV obtained by full-order optimal control. The resulting reduction in computing time was 52%. In general, the number of POD basis functions preserving a certain fixed level of relative energy increases during optimization, which speaks in favor of our nested reduced-order optimal control algorithm where we adapt the transformation matrix after simulating the full-order reservoir model with improved controls.

REFERENCES

[1] K. Aziz and A. Settari, *Petroleum reservoir simulation*, Applied Science Publishers, London, (1979).

[2] D.W. Peaceman, *Fundamentals of numerical reservoir simulation*, Elsevier Scientific Publishing Company, Amsterdam, (1977).

[3] H. Asheim, “Maximization of water sweep efficiency by controlling production and injection rates”, paper SPE 18365, in: Proc. SPE European Petroleum Conference, London, UK, (1988).

[4] B. Sudaryanto and Y.C. Yortsos, “Optimization of fluid front dynamics in porous media using rate control. I. Equal mobility fluids”, *Physics of Fluids,* **12** (7), 1656-1670, (2000).

[5] G.A. Virnovski, "Water flooding strategy design using optimal control theory", in: Proc. 6th European Symposium on IOR, Stavanger, Norway, 437-446, (1991).
[6] D.R. Brouwer and J.D. Jansen, "Dynamic optimisation of water flooding with smart wells using optimal control theory", *SPE Journal*, December, 391-402, (2004).
[7] P. Sarma, K. Aziz and L.J. Durlofsky: Implementation of adjoint solution for optimal control of smart wells. Paper SPE 92864 presented at the SPE Reservoir Simulation Symposium, Houston, USA, 31 January – 2 February (2005).
[8] P. Holmes, J.L. Lumley and G. Berkooz, *Turbulence, Coherent Structures, Dynamical Systems and Symmetry*, Cambridge University Press, (1996).
[9] K. Kunisch, and S. Volkwein, "Control of Burgers' equation by a reduced-order approach using proper orthogonal decomposition". *J. Optimization Theory and Applications* 1999; **102**: 345-371.
[10] S.S. Ravindran, "Reduced-order adaptive controllers for fluid flows using POD", *Journal of scientific computing*, **14**, 457-478, (2000).
[11] H.V. Ly and H.T. Tran, "Modeling and control of physical processes using proper orthogonal decomposition", *Mathematical and computer modeling,* **33**, 223-236, (2001).
[12] R.D. Prabhu, S.S. Collis and Y. Chang, "The influence of control on proper orthogonal decomposition of wall-bounded turbulent flows", *Physics of fluids*, **13**, 520-537, (2001).
[13] R. Gharbi, N. Smaoui, and E.J. Peters, "Prediction of unstable fluid displacements in porous media using the Karhunen-Loève decomposition". *In Situ* 1997; **21**: 331-356.
[14] R. Markovinović, E.L. Geurtsen, T. Heijn J.D. Jansen, "Generation of low-order reservoir models using POD, empirical gramians and subspace identification", in: Proc. 8th European Conf. On the Mathematics of Oil Recovery (ECMOR VIII), Freiberg, Germany, E31, 1-10, (2002).
[15] Heijn, T., Markovinović, R. and Jansen, J.D. "Generation of low-order reservoir models using system-theoretical concepts". *SPE Journal* 2004; **9**: 202-218.
[16] P.T.M. Vermeulen, A.W. Heemink and C.B.M. Te Stroet, "Reduced models for linear groundwater flow models using empirical orthogonal functions", *Advances in water resources,* 27, 54-69, (2004).
[17] J.F.M. van Doren, R. Markovinović, J.D. Jansen, "Reduced-order optimal control of water flooding using proper orthogonal decomposition", *Computational Geosciences*, published online. DOI: 10.1007/s10596-005-9014-2, (2006).
[18] R. Markovinović and J.D. Jansen, "Accelerating iterative solution methods using reduced-order models as solution predictors.", Int. J. for Numerical Methods in Engineering, published online, DOI: 10.1002/nme.1721, (2006).
[19] G.H. Golub and C. Van Loan, *Matrix computations*, John Hopkins Univ. Press, (1983).